JP Journal of Heat and Mass Transfer

http://www.pphmj.com
http://dx.doi.org/10.17654/HM014010029
Volume 14, Number 1, 2017, Pages 29-45 **ISSN: 0973-5763**

DUAL SOLUTIONS AND STABILITY ANALYSIS OF UNSTEADY STAGNATION-POINT FLOW AND HEAT TRANSFER OVER A SHRINKING SURFACE WITH RADIATION EFFECT

Ezad Hafidz Hafidzuddin[1], Roslinda Nazar[1] and Norihan Md. Arifin[2]

[1]School of Mathematical Sciences
Faculty of Science and Technology
Universiti Kebangsaan Malaysia
43600 UKM Bangi, Selangor
Malaysia

[2]Department of Mathematics and Institute for Mathematical Research
Universiti Putra Malaysia
43400 UPM Serdang, Selangor
Malaysia

Abstract

This paper deals with the study of unsteady stagnation-point boundary layer flow and heat transfer on a shrinking surface induced by a shrinking sheet in the presence of radiation effect. The governing nonlinear partial differential equations are reduced to a system of nonlinear ordinary differential equations using a similarity transformation. The transformed equations are solved numerically

Received: March 30, 2016; Accepted: May 17, 2016

Keywords and phrases: dual solutions, heat transfer, radiation effect, shrinking surface, stability analysis, unsteady flow.

using a “bvp4c” function in MATLAB. Dual solutions are found for a certain range of the unsteadiness parameters. A stability analysis has been performed to determine which solution is stable and physically realizable. The effects of the Prandtl number, unsteadiness, radiation and shrinking parameters on the skin friction coefficient and the local Nusselt number, as well as the velocity and temperature profiles are presented and discussed.

1. Introduction

Recently, the problem of boundary layer flow over a shrinking surface has become significantly important due to its wide applications in industries. As opposed to stretching sheet (where the velocity of the boundary is moving further from the origin), this new type of shrinking sheet flow is essentially a backward flow as discussed by Goldstein [1]. Miklavcic and Wang [2] were the first to investigate the flow induced by a shrinking sheet. On the other hand, Hiemenz [3] was the first to investigate the two-dimensional stagnation flow against a stationary semi-infinite wall, which then extended by Homann [4] by considering an axisymmetric case. Later, the problem of stagnation-point flow over a shrinking sheet/surface has been performed and extended by many researchers (see [5-7]).

All studies mentioned above consider the steady state problem, where the properties such as velocity and pressure do not depend upon time. However in certain aspects, flow becomes time dependent and thus, it is necessary to consider the unsteady flow condition. The studies of unsteady effects of boundary layer flow have been done by Riley [8]. Surma Devi et al. [9] studied the unsteady three-dimensional boundary layer flow over a stretching surface. Bhattacharyya [10] studied the unsteady stagnation-point flow over a shrinking sheet, while Fang et al. [11] investigated the unsteady viscous flow over a continuously shrinking surface with mass suction.

The introduction of radiation effects on the boundary layer flow and heat transfer opens a new research opportunity with many industrial and technological applications. Bhattacharyya [12] studied the effects of radiation and heat source/sink on the unsteady boundary layer flow and heat transfer

past a shrinking sheet with suction/injection. Midya [13] investigated the effect of radiation on heat transfer of an electrically conducting fluid flow over a linearly shrinking surface subject to heat sink and magnetic field applied normal to the plane of the flow, while Ali et al. [14] studied the problem of unsteady stagnation-point flow and heat transfer induced by a shrinking sheet in the presence of radiation effect. Recently, Sheikholeslami et al. [15] investigated the effect of thermal radiation on magnetohydrodynamics nanofluid flow and heat transfer by means of two phase model.

It is worth mentioning that the present study extends the problem done in [14] by analyzing the stability of the dual solutions obtained. The transformed ordinary differential equations are solved numerically using a "bvp4c" function from MATLAB. To the best of our knowledge, the stability analysis has never been considered for the present problem, therefore the reported results are new.

2. Mathematical Formulation

We consider the unsteady stagnation-point flow past a shrinking sheet which starts impulsively at time $t = 0$. Following [5], the unsteady potential stagnation-point flow at infinity is assumed to be $u_e(\bar{t},\, x) = ax(1 - \kappa\bar{t})^{-1}$ and $w_e(\bar{t},\, x) = az(1 - \kappa\bar{t})^{-1}$, where $\bar{t} = at$ is the non-dimensional time, a is the strength of the stagnation flow and κ is a parameter associated with the flow unsteadiness. For the stretching surface, the velocity is assumed to be $u_w(\bar{t},\, x) = b(x + c)(1 - \kappa\bar{t})^{-1}$ and $w_w(\bar{t},\, x) = 0$, where $b(> 0)$ is the stretching rate (shrinking if $b < 0$) and $-c$ is the location of the stretching origin. Under these assumptions, the unsteady boundary layer equations can be expressed as

$$\frac{\partial u}{\partial x} + \frac{\partial v}{\partial y} + \frac{\partial w}{\partial z} = 0, \tag{1}$$

$$\frac{\partial u}{\partial \bar{t}} + u\frac{\partial u}{\partial x} + v\frac{\partial u}{\partial y} + w\frac{\partial u}{\partial z} = -\frac{1}{\rho}\frac{\partial p}{\partial x} + \nu\frac{\partial^2 u}{\partial z^2}, \tag{2}$$

$$\frac{\partial v}{\partial \bar{t}} + u\frac{\partial v}{\partial x} + v\frac{\partial v}{\partial y} + w\frac{\partial v}{\partial z} = -\frac{1}{\rho}\frac{\partial p}{\partial y} + \nu\frac{\partial^2 v}{\partial z^2}, \tag{3}$$

$$\frac{\partial w}{\partial \bar{t}} + u\frac{\partial w}{\partial x} + v\frac{\partial w}{\partial y} + w\frac{\partial w}{\partial z} = -\frac{1}{\rho}\frac{\partial p}{\partial z} + \nu\frac{\partial^2 w}{\partial z^2}, \tag{4}$$

$$\frac{\partial T}{\partial \bar{t}} + u\frac{\partial T}{\partial x} + v\frac{\partial T}{\partial y} + w\frac{\partial T}{\partial z} = \frac{k}{\rho c_p}\frac{\partial^2 T}{\partial z^2} - \frac{1}{\rho c_p}\frac{\partial q_r}{\partial z}, \tag{5}$$

subject to the initial and boundary conditions

$$\bar{t} < 0 : u = v = w = 0,\ T = T_\infty \text{ for any } x, y, z,$$

$$\bar{t} \geq 0 : u = u_w(\bar{t}, x) = b(x+c)(1+\kappa\bar{t})^{-1},\ w = 0 = v_w(y, \bar{t}),\ T = T_w(x) \text{ at } z = 0,$$

$$u = u_e(\bar{t}, x) = ax(1-\kappa\bar{t})^{-1},\ v = 0 = v_e(\bar{t}, y) = 0,$$

$$w = w_e(\bar{t}, z) = -az(1-\kappa\bar{t})^{-1},\ T \to T_\infty \text{ as } z \to \infty, \tag{6}$$

where u, v and w are the velocity components along the x-, y- and z-axes, respectively, ρ is the fluid density, p is the pressure, ν is the kinematic viscosity, T is the non-dimensional temperature, $T_w(x)$ is the constant surface temperature, T_∞ is the ambient temperature and c_p is the specific heat of the fluid at a constant pressure. Using the Rosseland approximation for radiation (see Raptis et al. [16]), the radiative heat flux q_r is defined as

$$q_r = -\frac{4\sigma^*}{3k^*}\frac{\partial T^4}{\partial z}, \tag{7}$$

where σ^* and k^* are the Stefan-Boltzmann constant and the mean absorption coefficient, respectively. Following Bataller [17], we assume that the temperature differences within the flow such that the term T^4 can be expressed as a linear function of temperature. Expanding T^4 in a Taylor series about T^∞ and neglecting higher order terms, we have

$$T^4 \cong 4T_\infty^3 T - 3T_\infty^4. \tag{8}$$

Using (7) and (8), (5) becomes

$$\frac{\partial T}{\partial \bar{t}} + u\frac{\partial T}{\partial x} + v\frac{\partial T}{\partial y} + w\frac{\partial T}{\partial z} = \left(\beta + \frac{16\sigma^* T_\infty^3}{3\rho c_p k^*}\right)\frac{\partial^2 T}{\partial z^2}, \tag{9}$$

where $\beta = k/\rho c_p$ is the fluid thermal diffusivity. This equation shows that the effect of radiation is to enhance the thermal diffusivity. Let $N_R = 16\sigma^* T_\infty^3/3kk^*$ be the radiation parameter, which reduces (9) to

$$\frac{\partial T}{\partial \bar{t}} + u\frac{\partial T}{\partial x} + v\frac{\partial T}{\partial y} + w\frac{\partial T}{\partial z} = \beta(1 + N_R)\frac{\partial^2 T}{\partial z^2}. \tag{10}$$

Introducing the following similarity transformations (see [5] and [9]):

$$u = (1 - \kappa\bar{t})^{-1}(axf'(\eta) + bcg(\eta)),\ v = 0,\ w = -\sqrt{a\nu}(1 - \kappa\bar{t})^{-1/2} f(\eta),$$

$$\theta(\eta) = (T - T_\infty)/(T_w - T_\infty),\ \eta = \sqrt{a/\nu}(1 - \kappa\bar{t})^{-1/2} z. \tag{11}$$

Substituting (11) into (2), (3) and (10) results in the following ordinary differential equations:

$$f''' + ff'' - f'^2 + 1 - M(f' + \eta f''/2 - 1) = 0, \tag{12}$$

$$g'' + fg' - f'g - M(g + \eta g'/2) = 0, \tag{13}$$

$$\left(\frac{1 + N_R}{\Pr}\right)\theta'' + f\theta' - M\eta\theta'/2, \tag{14}$$

and the boundary conditions (6) become

$$f(0) = 0,\ f'(0) = \varepsilon,\ g(0) = 1,\ \theta(0) = 1,$$

$$f'(\eta) = 1,\ g(\eta) = 0,\ \theta(\eta) = 0 \text{ as } \eta \to \infty, \tag{15}$$

where $M = \lambda/a$ is the unsteadiness parameter, $\Pr = \nu/\alpha$ is the Prandtl number and $\varepsilon = b/a$ is the shrinking $(\varepsilon < 0)$ parameter. Meanwhile, the pressure p can be written as

$$\frac{p}{\rho} = \frac{p_0}{\rho} - \frac{1}{2}\left(\frac{ax}{1-\kappa t}\right)^2 - \frac{w^2}{2} + \nu\frac{\partial w}{\partial z} + \frac{\partial}{\partial t}\int_z^\infty w dz, \tag{16}$$

where p_0 is the stagnation pressure. It is worth mentioning that the thermal radiation's effect is ignored by setting $N_R = 0$ in equation (14).

The physical quantities of interest are the skin friction coefficient C_f and the local Nusselt number Nu_x, which are given by

$$C_f = \tau_w/\rho u_e^2, \quad Nu_x = xq_w/k(T_w - T_\infty). \tag{17}$$

The skin friction τ_w and the heat flux q_w are expressed as

$$\tau_w = \mu\left(\frac{\partial u}{\partial z}\right)_{z=0}, \quad q_w = -k\left(\frac{\partial T}{\partial z}\right)_{z=0}, \tag{18}$$

where μ and k are the dynamic viscosity and thermal conductivity, respectively. Using (11), (17) and (18), we obtain

$$\mathrm{Re}_x^{1/2} C_f = f''(0) + (bc/u_e)g'(0), \quad \mathrm{Re}_x^{-1/2} Nu_x = -\theta'(0), \tag{19}$$

where $\mathrm{Re}_x = u_w x/\nu$ is the local Reynolds number based on the shrinking sheet velocity u_w.

3. Stability Analysis

In the Introduction section earlier, we have mentioned the existence of dual solutions. In order to determine which of these solutions are stable and physically realizable in the real world applications, a stability analysis needs to be performed. This analysis has been done by Weidman et al. [18], Harris et al. [19], Weidman and Sprague [20], Roşca and Pop [21] and recently by Nazar et al. [22], Ishak [23] and Hafidzuddin et al. [24], among others.

Following [18], we begin by introducing a new dimensionless time variable τ, which is associated with an initial value problem and consistent

with the question of which solution (branch) will be obtained in practice (physically realizable). With the introduction of τ and (11), we have

$$u = (1-\kappa\bar{t})^{-1}(axf'(\eta,\tau)+bcg(\eta,\tau)),\ v=0,\ w-\sqrt{a\nu}(1-\kappa\bar{t})^{-1/2}\,f(\eta,\tau),$$

$$\theta(\eta,\tau)=(T-T_\infty)/(T_w-T_\infty),\ \eta=\sqrt{a/\nu}(1-\kappa\bar{t})^{-1/2}z,\ \tau=a\bar{t}(1-\kappa\bar{t})^{-1}. \quad (20)$$

Substituting (20) into (2), (3) and (10), we obtain

$$\frac{\partial^3 f}{\partial\eta^3}+f\frac{\partial^2 f}{\partial\eta^2}-\left(\frac{\partial f}{\partial\eta}\right)^2+1-M\left(\frac{\partial f}{\partial\eta}+\frac{\eta}{2}\frac{\partial^2 f}{\partial\eta^2}-1\right)-(1+M\tau)\frac{\partial^2 f}{\partial\eta\partial\tau}=0, \quad (21)$$

$$\frac{\partial^2 g}{\partial\eta^2}+f\frac{\partial g}{\partial\eta}-\frac{\partial f}{\partial\eta}g-M\left(g+\frac{\eta}{2}\frac{\partial g}{\partial\eta}\right)-(1+M\tau)\frac{\partial g}{\partial\tau}=0, \quad (22)$$

$$\left(\frac{1+N_R}{\mathrm{Pr}}\right)\frac{\partial^2\theta}{\partial\eta^2}+\left(f-M\frac{\eta}{2}\right)\frac{\partial\theta}{\partial\eta}-(1+M\tau)\frac{\partial\theta}{\partial\tau}=0, \quad (23)$$

subject to the boundary conditions

$$f(0,\tau)=0,\ \frac{\partial f}{\partial\eta}(0,\tau)=\varepsilon,\ g(0,\tau)=1,\ \theta(0,\tau)=1,$$

$$\frac{\partial f}{\partial\eta}(\eta,\tau)=1,\ g(\eta,\tau)=0,\ \theta(\eta,\tau)=0 \text{ as } \eta\to\infty. \quad (24)$$

In order to determine the stability of the solution $f=f_0(\eta)$, $g=g_0(\eta)$ and $\theta=\theta_0(\eta)$ satisfying the boundary value problem (12)-(15), we write (see [18] and [21])

$$f(\eta,\tau)=f_0(\eta)+e^{-\xi\tau}F(\eta,\tau),\quad g(\eta,\tau)=g_0(\eta)+e^{-\xi\tau}G(\eta,\tau),$$

$$\theta(\eta,\tau)=\theta_0(\eta)+e^{-\xi\tau}T(\eta,\tau), \quad (25)$$

where ξ is an unknown eigenvalue parameter, and $F(\eta,\tau)$, $G(\eta,\tau)$ and $T(\eta,\tau)$ are small relative to $f_0(\eta)$, $g_0(\eta)$ and $\theta_0(\eta)$, respectively.

Solutions of the eigenvalue problem (21)-(24) give an infinite set of eigenvalues $\xi_1 < \xi_2 < \xi_3 \ldots$; if the smallest eigenvalue ξ_1 is positive, there is an initial decay which indicates that the flow is stable; however, if ξ_1 is negative, then there is an initial growth of disturbances which indicates that the flow is unstable (see [20]).

Substituting (25) into (21)-(23) yields the following linearized problem:

$$\frac{\partial^3 F}{\partial \eta^3} + f_0 \frac{\partial^2 F}{\partial \eta^2} + f_0'' F(-2 f_0' - \xi) \frac{\partial F}{\partial \eta} - M\left(\frac{\partial F}{\partial \eta} + \frac{\eta}{2} \frac{\partial^2 F}{\partial \eta^2}\right) - \frac{\partial^2 F}{\partial \eta \partial \tau} = 0, \quad (26)$$

$$\frac{\partial^2 G}{\partial \eta^2} + f_0 \frac{\partial G}{\partial \eta} + F g_0' - (f_0' - \xi) G - g_0 \frac{\partial F}{\partial \eta} - M\left(G + \frac{\eta}{2} \frac{\partial G}{\partial \eta}\right) - \frac{\partial G}{\partial \tau} = 0, \quad (27)$$

$$\left(\frac{1 + N_R}{\mathrm{Pr}}\right) \frac{\partial^2 T}{\partial \eta^2} + F \theta_0' + \xi T + \left(f_0 - M \frac{\eta}{2}\right) \frac{\partial T}{\partial \eta} - \frac{\partial T}{\partial \tau} = 0, \quad (28)$$

subject to the following boundary conditions:

$$F(0, \tau) = 0, \frac{\partial F}{\partial \eta}(0, \tau) = \varepsilon, G_0(0, \tau) = 0, T_0(0, \tau) = 0,$$

$$\frac{\partial F}{\partial \eta}(\eta, \tau) \to 0, G_0(\eta, \tau) \to 0, T_0(\eta, \tau) \to 0 \text{ as } \eta \to \infty. \quad (29)$$

Following Weidman et al. [18], we investigate the stability of the steady flow $f_0(\eta)$, $g_0(\eta)$ and $\theta_0(\eta)$ by setting $\tau = 0$. Hence, $F = F_0(\eta)$, $G = G_0(\eta)$ and $T = T_0(\eta)$ in (26)-(28) identify the initial growth or decay of the solution (25). To test our numerical procedure, we have to solve the linear eigenvalue problem

$$F_0''' + f_0 F_0'' - f_0'' F_0 - (2 f_0' - \xi) F_0' - M(F_0' + \eta F_0''/2) = 0, \quad (30)$$

$$G_0'' + f_0 G_0' - F_0 g_0' - (f_0' - \xi) G_0 - g_0 F_0' - M(G_0 + \eta G_0') = 0, \quad (31)$$

$$\left(\frac{1 + N_R}{\mathrm{Pr}}\right) T_0'' + F_0 \theta_0' + \xi T_0 + (f_0 - M\eta/2) T_0' = 0, \quad (32)$$

along with the boundary conditions

$$F_0(0) = 0,\ F_0'(0) = 0,\ G_0(0) = 0,\ T_0(0) = 0,$$

$$F_0'(\eta) = 0,\ G_0(\eta) \to 0,\ T_0(\eta) \to 0 \ \text{ as } \ \eta \to \infty. \tag{33}$$

Following [19], we determine the range of possible eigenvalues by relaxing a boundary condition on $F_0(\eta)$, $G_0(\eta)$ or $T_0(\eta)$. For the present problem, we relax the condition $F_0'(\eta) \to 0$ and replace it with a new condition $F_0''(0) = 1$.

4. Results and Discussion

The nonlinear ordinary differential equations (12)-(14) along with the boundary conditions (15) were solved numerically using the "bvp4c" function from MATLAB (see Kierzenka and Shampine [25]) for some values of the governing parameters, which are the unsteadiness parameter M, shrinking parameter ε, Prandtl number Pr and radiation parameter N_R. The dual (upper and lower branches) solutions are obtained by setting different initial guesses for the missing values of $f''(0)$, $g'(0)$ and $-\theta'(0)$. The guesses must satisfy the boundary conditions (15) and keep the behavior of the solution. To verify the accuracy of the results obtained, comparisons for the numerical values of $f''(0)$, $g'(0)$ and $-\theta'(0)$ when $A = 0$, $\text{Pr} = 0.7$ and are $N_R = 0$ made with [14], as can be seen in Table 1. The comparisons are found to be in excellent agreement, hence we are confident that the present numerical method is accurate.

Table 1. Comparison of the values for $f''(0)$, $g'(0)$ and $-\theta'(0)$ with [14] when $A = 0$, $\Pr = 0.7$ and $N_R = 0$

	Ali et al. [14]			Present results		
ε	$f''(0)$	$g'(0)$	$-\theta'(0)$	$f''(0)$	$g'(0)$	$-\theta'(0)$
–0.25	1.40224	–0.66857	0.44340	1.40224	–0.66857	0.44340
–0.5	1.49567	–0.50145	0.38439	1.49567	–0.50145	0.38439
–0.75	1.48930	–0.29376	0.31547	1.48930	–0.29376	0.31547
–1	1.32882	0	0.22833	1.32882	0	0.22833

The variations of the reduced skin friction coefficient $f''(0)$ and the reduced local Nusselt number $-\theta'(0)$ with the unsteadiness parameter M for some values of shrinking parameter ε and radiation parameter N_R are presented in Figures 1 and 2, respectively. The dual solutions exist for a certain range of M, which is when $M < 0$. It can be seen that there is no solution for $M < M_c$, where M_c represents the critical value of M. It is worth mentioning here that beyond these critical points, the solutions based upon the boundary layer approximations are not possible due to the separation of the boundary layer from the surface.

Figure 1 displays the variations of $f''(0)$ for some values of the shrinking parameter ε when $N_R = 3$ and $\Pr = 0.7$. It can be observed that the values of $f''(0)$ increase with the decrease of $|\varepsilon|$. We also notice that the critical values of $|M_c|$ increase with the decrease of $|\varepsilon|$. Hence, the shrinking parameter ε widen the range of unsteadiness parameter M for which solutions exist. Meanwhile, Figure 2 shows the variations of $-\theta'(0)$ for some values of radiation parameter N_R when $\varepsilon = -0.5$ and $\Pr = 0.7$. It is shown that the values of $-\theta'(0)$ increase with the decrease of M. We notice that the increase of N_R reduces the heat transfer rate at the surface.

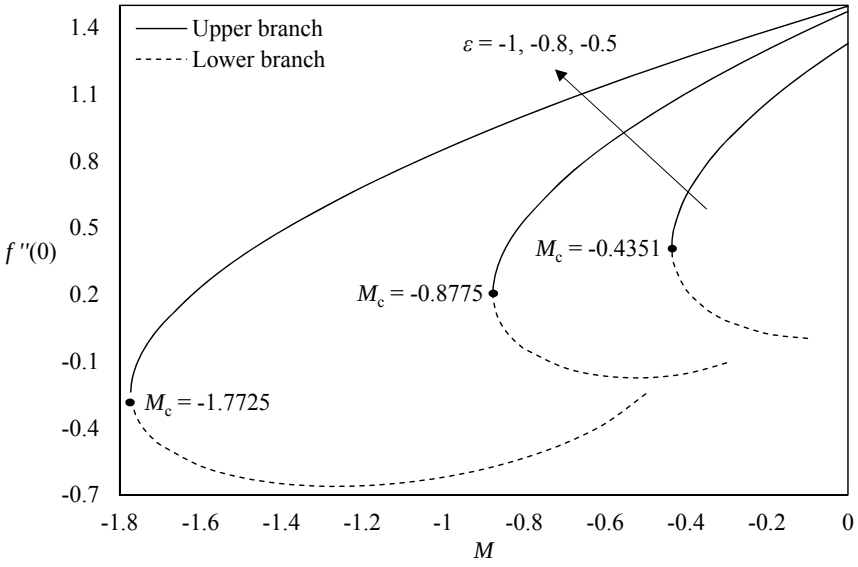

Figure 1. Variations of $f''(0)$ with M for different values of ε when $N_R = 3$ and $\Pr = 0.7$.

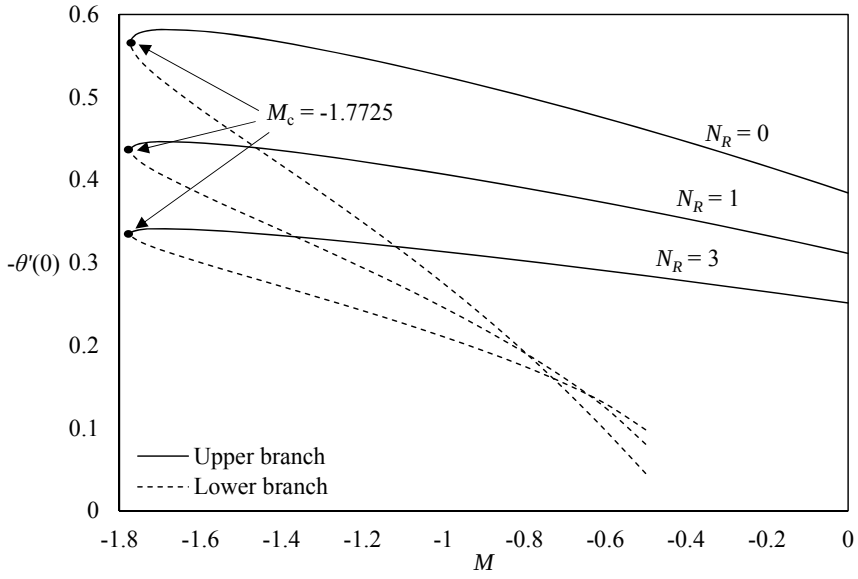

Figure 2. Variation of $-\theta'(0)$ with M for different values of N_R when $\varepsilon = -0.5$ and $\Pr = 0.7$.

Velocity profiles $f'(\eta)$ and $g(\eta)$ for some values of the shrinking parameter ε when $M = -0.7$, $\Pr = 0.7$ and $N_R = 3$ are given in Figures 3 and 4, respectively. The profiles of $f'(\eta)$ are seen to decrease, while $g(\eta)$ is seen to increase with the increase of $|\varepsilon|$. Here, the oscillatory behavior is observed on the velocity profile $g(\eta)$ with the large values of $|\varepsilon|$. Figure 5 illustrates the temperature profiles $\theta(\eta)$ for different values of the radiation parameter N_R and the Prandtl number Pr when $\varepsilon = -0.5$ and $M = -0.7$. The profiles, as well as the thermal boundary layer thicknesses are seen to decrease with the decrease of N_R and with the increase of Pr. Physically, as Pr increases, the thermal fluid conductivity decreases, which in turn reduces conduction, causing the thermal boundary layer thickness to become smaller. It can be observed from Figures 3-5 that the boundary layer thickness for the lower branch is always larger than the upper branch. All velocity and temperature profiles presented in this study satisfy the far field boundary conditions (15) asymptotically, hence supporting the numerical results obtained.

A stability analysis was performed by solving an unknown eigenvalue ξ_1 on equations (30)-(32), along with the boundary conditions (33) to determine which of the branch is stable. The computation is done by using the same method, which is "bvp4c" function. Table 2 presents the smallest eigenvalues for ξ_1 some values of ε and M. From the table, it is observed that the upper branch solutions have positive eigenvalues ξ_1, while the lower branch solutions have negative eigenvalues ξ_1, and thus we conclude that the first (upper branch) solution is stable while the second (lower branch) solution is unstable.

Table 2. Smallest eigenvalue ξ_1 for some values of ε and M when $\mathrm{Pr} = 0.7$, $N_R = 3$

ε	M	ξ_1 (upper)	ξ_1 (lower)
–0.5	–1.77	0.1762	–0.1751
	–1.75	0.2449	–0.2391
–0.8	–0.87	0.1573	–0.1542
	–0.85	0.3027	–0.2913
–1	–0.43	0.1379	–0.1350
	–0.4	0.3665	–0.3465

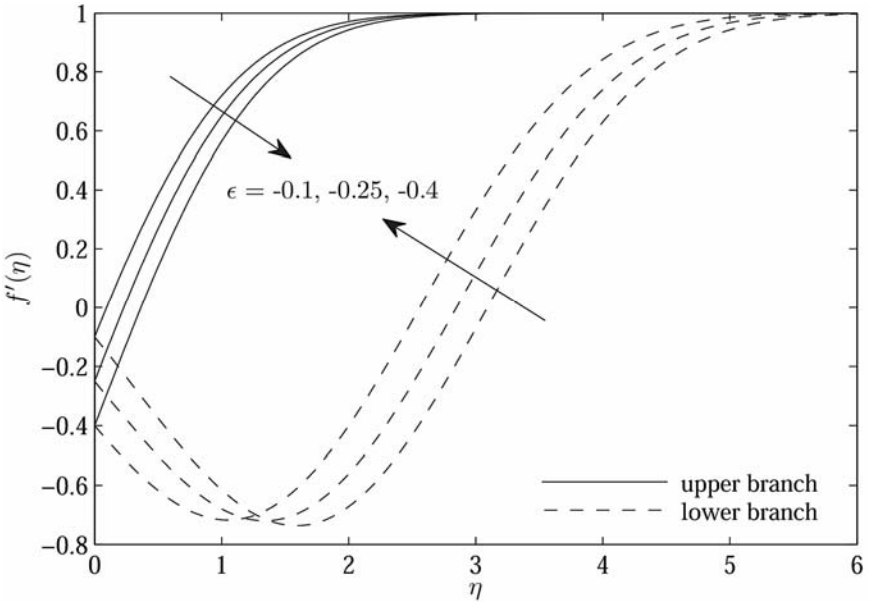

Figure 3. Velocity profiles $f'(\eta)$ for different values of ε when and $M = -0.7$, $\mathrm{Pr} = 0.7$ and $N_R = 3$.

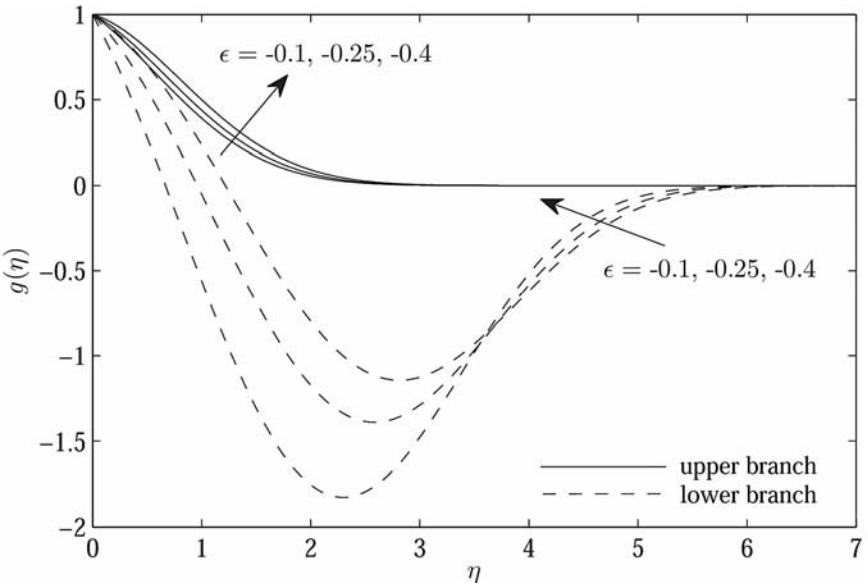

Figure 4. Velocity profiles $g(\eta)$ for different values of ε when $M = -0.7$, $\mathrm{Pr} = 0.7$ and $N_R = 3$.

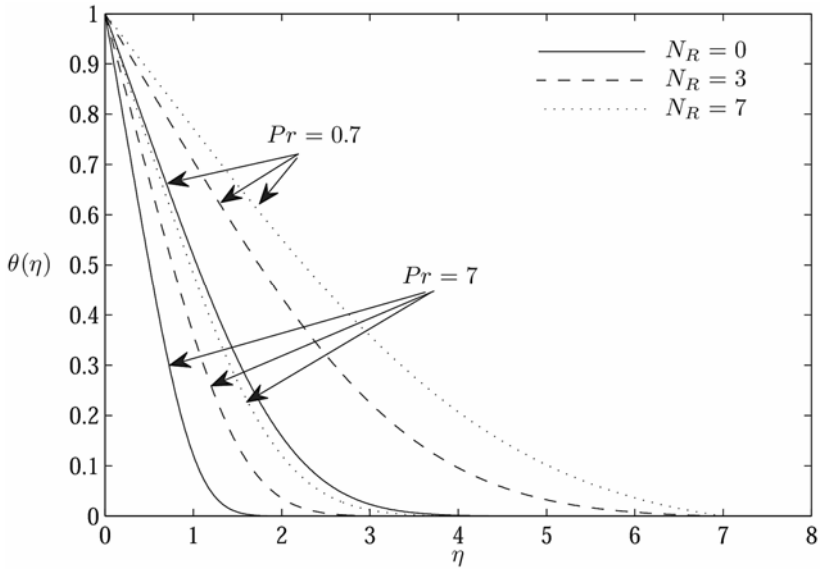

Figure 5. Temperature profiles $\theta(\eta)$ for different values of N_R and Pr when $M = -0.7$ and $\varepsilon = -0.5$.

5. Conclusions

A numerical study is performed for the problem of unsteady stagnation-point flow and heat transfer on a shrinking surface induced by a shrinking sheet in the presence of radiation effect. The numerical computation was performed by using the "bvp4c" function in MATLAB. The numerical results obtained were compared with the previous literature and the comparison was found to be in excellent agreement. Dual solutions were found for a certain range of the unsteadiness parameters. It is found that the increase of the radiation parameter reduced the heat transfer rate at the surface. The shrinking parameter widened the range of the unsteadiness parameter for which solutions existed. The thermal boundary layer thickness is found to decrease with the decrease of the unsteadiness and shrinking parameters and with the increase of the radiation parameter and Prandtl number. Stability analysis is performed and concluded that the first (upper branch) solution was stable while the second (lower branch) solution was not.

Acknowledgment

The authors gratefully acknowledged the financial support received in the form of fundamental research grant (FRGSTOPDOWN/2014/SG04/ UKM/01/1) from the Ministry of Higher Education, Malaysia, and research university grant (GP-K007136) from the Universiti Kebangsaan Malaysia.

References

[1] S. Goldstein, On backward boundary layers and flow in converging passages, J. Fluid Mech. 21(1) (2006), 33-45.

[2] M. Miklavcic and C. Y. Wang, Viscous flow due to a shrinking sheet, Quart. Appl. Math. 64 (2006), 283-290.

[3] K. Hiemenz, Die Grenzschicht an einem in den gleichformingen flussigkeitsstrom eingetauchten graden krei-szylinder, Dingler's Polytech. J. 326 (1911), 321-324.

[4] F. Homann, Der Einfluß großer Zähigkeit bei der Strömung um den Zylinder und um die Kugel, ZAMM-Zeitschrift für Angew. Math. und Mech. 16(3) (1936), 153-164.

[5] C. Y. Wang, Stagnation flow towards a shrinking sheet, Internet. J. Non-Linear. Mech. 43(5) (2008), 377-382.

[6] F. Aman, A. Ishak and I. Pop, Magnetohydrodynamic stagnation-point flow towards a stretching/shrinking sheet with slip effects, Int. Commun. Heat Mass Transf. 47 (2013), 68-72.

[7] N. Najib, N. Bachok, N. M. Arifin and A. Ishak, Boundary layer stagnation point flow and heat transfer past a permeable exponentially shrinking cylinder, Int. J. Math. Model. Methods Appl. Sci. 8(1) (2014), 121-126.

[8] N. Riley, Unsteady viscous flows, Sci. Prog. 74 (1990), 361-377.

[9] C. D. Surma Devi, H. S. Takhar and G. Nath, Unsteady, three-dimensional, boundary-layer flow due to a stretching surface, Int. J. Heat Mass Transf. 29(12) (1986), 1996-1999.

[10] K. Bhattacharyya, Dual solutions in unsteady stagnation-point flow over a shrinking sheet, Chinese Phys. Lett. 28(8) (2011), 084702.

[11] T.-G. Fang, J. Zhang and S.-S. Yao, Viscous flow over an unsteady shrinking sheet with mass transfer, Chinese Phys. Lett. 26(1) (2009), 14703.

[12] K. Bhattacharyya, Effects of radiation and heat source/sink on unsteady MHD boundary layer flow and heat transfer over a shrinking sheet with suction/injection, Front. Chem. Eng. China 5(3) (2011), 376-384.

[13] C. Midya, Heat transfer in MHD boundary layer flow over a shrinking sheet with radiation and heat sink, J. Glob. Res. Math. Arch. 1(2) (2013), 63-70.

[14] F. M. Ali, R. Nazar, N. M. Arifin and I. Pop, Unsteady stagnation-point flow towards a shrinking sheet with radiation effect, Int. Sch. Sci. Res. Innov. 8(5) (2014), 755-759.

[15] M. Sheikholeslami, D. D. Ganji, M. Y. Javed and R. Ellahi, Effect of thermal radiation on magnetohydrodynamics nanofluid flow and heat transfer by means of two phase model, J. Magn. Magn. Mater. 374 (2015), 36-43.

[16] A. Raptis, C. Perdikis and H. S. Takhar, Effect of thermal radiation on MHD flow, Appl. Math. Comput. 153(3) (2004), 645-649.

[17] R. C. Bataller, Similarity solutions for flow and heat transfer of a quiescent fluid over a nonlinearly stretching surface, J. Mater. Process. Technol. 203(1-3) (2008), 176-183.

[18] P. D. Weidman, D. G. Kubitschek and A. M. J. Davis, The effect of transpiration on self-similar boundary layer flow over moving surfaces, Int. J. Eng. Sci. 44(11-12) (2006), 730-737.

[19] S. D. Harris, D. B. Ingham and I. Pop, Mixed convection boundary-layer flow near the stagnation point on a vertical surface in a porous medium: Brinkman model with slip, Transp. Porous Media 77(2) (2009), 267-285.

[20] P. D. Weidman and M. A. Sprague, Flows induced by a plate moving normal to stagnation-point flow, Acta Mech. 219(3-4) (2011), 219-229.

[21] A. V. Roşca and I. Pop, Flow and heat transfer over a vertical permeable stretching/shrinking sheet with a second order slip, Int. J. Heat Mass Transf. 60 (2013), 355-364.

[22] R. Nazar, A. Noor, K. Jafar and I. Pop, Stability analysis of three-dimensional flow and heat transfer over a permeable shrinking surface in a Cu-water nanofluid, Int. J. Math. Comput. Phys. Quantum Eng. 8(5) (2014), 776-782.

[23] A. Ishak, Flow and heat transfer over a shrinking sheet: a stability analysis, Int. J. Mech. Aerospace, Ind. Mechatronics Eng. 8(5) (2014), 901-905.

[24] E. H. Hafidzuddin, R. Nazar, N. M. Arifin and I. Pop, Stability analysis of unsteady three-dimensional viscous flow over a permeable stretching/shrinking surface, J. Qual. Meas. Anal. 11(1) (2015), 19-31.

[25] J. Kierzenka and L. F. Shampine, A BVP solver based on residual control and the Matlab PSE, ACM Trans. Math. Softw. 27(3) (2001), 299-316.